HEAT TRANSFER FROM A ROTATING CIRCULAR CYLINDER IN THE STEADY REGIME: EFFECTS OF PRANDTL NUMBER

by

Varun SHARMA and Amit Kumar DHIMAN*

Department of Chemical Engineering, Indian Institute of Technology Roorkee,

Roorkee – 247 667, India

In this work, effects of Prandtl number on the heat transfer characteristics of an unconfined rotating circular cylinder are investigated for varying rotation rate (α = 0 - 5) in the Reynolds number range 1 - 35 and Prandtl numbers range 0.7 – 100 in the steady flow regime. The numerical calculations are carried out by using a finite volume method based commercial CFD solver FLUENT. The isotherm patterns are presented for varying values of Prandtl number and rotation rate in the steady regime. The variation of the local and the average Nusselt numbers with Reynolds number, Prandtl number and rotation rate are presented for the above range of conditions. The average Nusselt number is found to decrease with increasing value of the rotation rate for the fixed value of the Reynolds and Prandtl numbers. With increasing value of the Prandtl number, the average Nusselt number increases for the fixed value of the rotation rate and the Reynolds number; however, the larger values of the Prandtl numbers show a large reduction in the value of the average Nusselt number with increasing rotation rate.

Key words: *steady regime, rotating circular cylinder, Prandtl number, Nusselt number, rotation rate*

1. Introduction

Forced convective heat transfer from rotating cylinders has been a subject of great interest for researchers due to its high applicability in various industrial processes. The applications may include cylindrical cooling devices in plastics and glass industries, contact cylinder driers in paper making, textile, food processing and chemical processing industries, etc. Despite the configuration being simple, the flow around a rotating cylinder involves complex transport phenomenon because of many factors such as the effect of cylinder rotation on the production of lift force and moment, evolution of surrounding temperature field, etc. This work is concerned with the heat transfer from a rotating cylinder for varying values of Prandtl numbers in the steady regime.

*Corresponding author; e-mails: dhimuamit@rediffmail.com; amitdfch@iitr.ernet.in

Tel.: +91-9410329605 (M), +91-1332-285890 (O)

In literature, sufficient amount of information is available regarding the effects of Prandtl number on the heat transfer from a stationary circular cylinder [1 - 7]. The effect of Prandtl number on the heat transfer from a cylinder in the cross-flow configuration has been investigated by Dennis *et al.* [3] by varying Prandtl number up to 3.3×10^4 and Reynolds number up to 40. The above ranges of values are extended by Chang and Finlayson [4] for Re up to 150 and Pr up to 10^4. The experimental results have been presented for uniform heat flux condition for different values of Prandtl number by varying air, water and ethylene glycol as mediums with varying concentrations and Reynolds number in the range 10^3 - 10^5 [5]. Subsequently, they [6] studied the local and average heat transfer characteristics around a circular cylinder for the Reynolds number range 2×10^3 - 9×10^4 and Prandtl number range 0.7 - 176. Three regions of flow: laminar boundary layer, reattachment of shear layer and periodic vortex regions are indicated around the cylinder for sub-critical flow. The Nusselt number in each region strongly depends on the Reynolds number and the Prandtl number with different power indices. Bharti *et al.* [7] investigated the effects of Reynolds number, Prandtl number and thermal boundary conditions (uniform heat flux and constant wall temperature) around the cylinder for the range $10 \le \mathrm{Re} \le 45$ and $0.7 \le \mathrm{Pr} \le 400$ in the steady regime. The rate of heat transfer is found to increase with an increase in Reynolds and/or Prandtl numbers.

In contrast, for the problem under consideration, most of the available information in the open literature is limited to the flow and heat transfer for the working fluid as air (i.e., $\mathrm{Pr} = 0.7$). Badr *et al.* [8] presented the limiting results for the steady flow at Re = 5 and 20 (α = 0.1 – 1.0) and some unsteady results for Re = 60, 100 and 200. Ingham and Tang [9] obtained the numerical solutions for steady uniform flow past a rotating cylinder for the Reynolds numbers of 5 and 20 for $0 \le \alpha \le 3$. The particular attention has been given to the quantities such as drag and lift coefficients since they are very sensitive to the method of solution. Kang *et al.* [10] investigated numerically the laminar flow round a rotating cylinder for Re = 60, 100, 160 and α = 0 – 2.5 and reported that an increase in the rotation rate leads to the decrease in the mean drag and the linear increase in the mean lift. Stojkovic *et al.* [11] studied the effect of rotation rate on the flow around a rotating cylinder in the range $0 \le \alpha \le 6$ with Reynolds number varying from 0.01 – 45 in the steady regime; further, unsteady flow calculations are carried out for Re = 100 and α = 0 – 2. The rotation of the cylinder suppresses the vortex development in both steady and unsteady flow regimes and significantly changes the flow field close to the cylinder. For very low Reynolds numbers, the drag force is not affected by rotation and the lift force is a linear function of rotation. Mittal and Kumar [12] examined the flow past a rotating cylinder for a fixed Reynolds number of 200 and rotation rate varying from 0 - 5. The vortex shedding is observed for $\alpha < 1.91$. For higher rotation rates, the flow is found to achieve a steady state, except for $4.34 < \alpha < 4.70$ where the flow becomes unstable again. It is proposed that for large rotation rates, very large lift coefficients can be obtained via the Magnus effect. Recently, Panda and Chhabra [13] investigated the flow of non-Newtonian power-law fluids past a rotating cylinder in the range Re = 0.1 – 40, α = 0 – 6 and power-law index = 0.2 – 1 in the steady regime.

The flow and heat transfer over an isothermal cylinder is investigated by Badr and Dennis [14] for the range Re = 5 – 100 for a fixed Prandtl number of 0.7. They found a decrease in the laminar forced convection heat transfer on increasing α for $\alpha \le 4$. Mahfouz

and Badr [15] investigated the problem of laminar heat convection from a circular cylinder performing steady rotation for Rayleigh numbers up to 10^4 and Reynolds numbers (based on surface velocity) up to 400 for two Prandtl numbers of 0.7 and 7. The rate of heat transfer found to increase with the increase of Rayleigh number and decrease with the increase of speed of rotation. The increase of Prandtl number resulted in an appreciable increase in the average Nusselt number only at low Reynolds numbers. Yan and Zu [16] proposed a lattice Boltzmann Method (LBM) approach for the numerical simulation of heat transfer and fluid flow past a rotating isothermal cylinder for Re = 200, Pr = 0.5 and 1. The numerical results, such as velocity and temperature distributions and lift and drag coefficients, agreed well with those reported in the literature. Kendoush [17] employed a boundary layer approach in order to predict the value of the Nusselt number for a rotating cylinder. Recently, the flow and heat transfer around a rotating circular cylinder is studied by Paramane and Sharma [18] for the values of α varies from 0 - 6 for Reynolds number range 20 - 160 for a fixed value of the Prandtl number of 0.7. The values of drag coefficient as well as average Nusselt number are found to decrease on increasing the rotation rate. Subsequently, Paramane and Sharma [19] investigated the free stream flow and forced convection heat transfer across a rotating cylinder, dissipating uniform heat flux, for identical range of Re, α and Pr [18]. At higher rotational velocity, the Nusselt number is almost independent of Reynolds number and thermal boundary conditions. Nobari and Ghazanfarian [20] studied the convective heat transfer from a rotating cylinder with inline oscillation at Reynolds numbers of 100, 200 and 300. Different rotational speeds of the cylinder (0 – 2.5) are considered at various oscillating amplitudes and frequencies with three different Prandtl numbers of 0.7, 6 and 20. As the rotational speed of the cylinder increases, both the Nusselt number and the drag coefficient decrease rapidly. Nemati et al. [21] investigated the laminar flow and heat transfer from a rotating circular cylinder with uniform planar shear, where the free stream velocity varies linearly across the cylinder using Multi-Relaxation-Time (MRT) lattice Boltzmann method. The effects of variation of Reynolds number, rotational speed ratio at shear rate 0.1, blockage ratio 0.1 and Prandtl number 0.71 are studied. The Reynolds number changing from 50 to 160 for three rotational speed ratios of 0, 0.5 and 1 is investigated. They reported that the rotation of the cylinder pushes forward the point of flow separation, hence, the minimum point of Nusselt number distribution on the cylinder surface shifts to the right.

Yoon et al. [22] examined the laminar forced convection heat transfer past two rotating circular cylinders in a side-by-side arrangement at various range of absolute rotational speeds ($|\alpha| \le 2$) for different gap spacings at the Reynolds number of 100 and a fixed Prandtl number of 0.7. As $|\alpha|$ increases, the behavior of time- and space- averaged Nusselt number has the decaying pattern for all the gap spacings considered. Moshkin and Sompong [23] investigated the two-dimensional heat transfer from two rotating circular cylinders in cross-flow of incompressible fluid under isothermal boundary condition for Reynolds numbers up to 40, while Prandtl number ranges between 0.7 and 50. The increase of Prandtl number resulted in an appreciable increase in the average Nusselt number.

Thus, based upon the above discuss and as far as known to us, it can be concluded here that no work is available regarding the effects of Prandtl numbers on the heat transfer across a rotating circular cylinder with varying Prandtl numbers in the steady regime. Hence,

the objectives of the present study are to investigate the effects of Prandtl number on the heat transfer across a rotating circular cylinder and to fill this gap in the literature.

2. Problem Statement, governing equations and boundary conditions

The system here consists of a two-dimensional infinite long circular cylinder (Fig. 1) having diameter D which is maintained at a constant temperature of T_w^* and is rotating in a counter-clockwise direction with a constant angular velocity of ω. It is exposed to a constant free stream velocity of U_∞ at a uniform temperature of T_∞ at the inlet. As the temperature difference between the streaming liquid and the surface of the cylinder is small (= 2K), therefore the variation of physical properties, particularly density and viscosity, with temperature could be neglected.

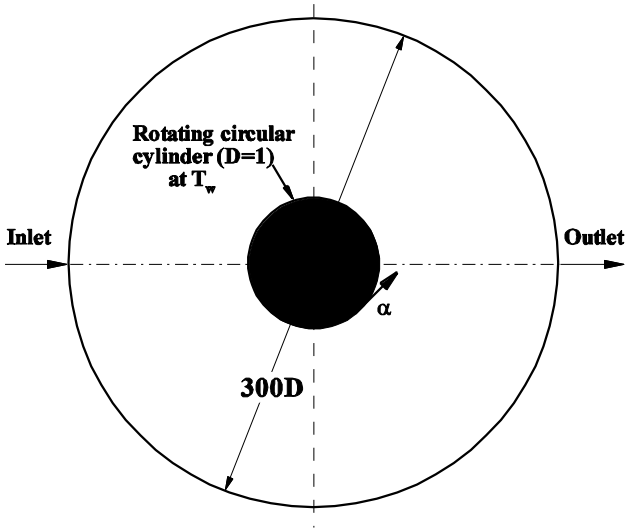

Figure 1: Schematics of the unconfined flow and heat transfer around a rotating (counter-clock wise) circular cylinder

The governing partial differential equations here are the dimensionless form of Navier-Stokes and energy equations in two dimensions for the incompressible flow around a rotating circular cylinder.

Continuity equation

$$\frac{\partial U}{\partial X}+\frac{\partial V}{\partial Y}=0 \tag{1}$$

X- Momentum equation

$$\frac{\partial U}{\partial \tau}+\frac{\partial (UU)}{\partial X}+\frac{\partial (VU)}{\partial Y}=-\frac{\partial p}{\partial X}+\frac{1}{\mathrm{Re}}\left(\frac{\partial^2 U}{\partial X^2}+\frac{\partial^2 U}{\partial Y^2}\right) \tag{2}$$

Y- Momentum equation

$$\frac{\partial V}{\partial \tau}+\frac{\partial (UV)}{\partial X}+\frac{\partial (VV)}{\partial Y}=-\frac{\partial p}{\partial Y}+\frac{1}{\mathrm{Re}}\left(\frac{\partial^2 V}{\partial X^2}+\frac{\partial^2 V}{\partial Y^2}\right) \quad (3)$$

Energy equation

$$\frac{\partial \theta}{\partial \tau}+\frac{\partial (U\theta)}{\partial X}+\frac{\partial (V\theta)}{\partial Y}=\frac{1}{\mathrm{Re}\,\mathrm{Pr}}\left(\frac{\partial^2 \theta}{\partial X^2}+\frac{\partial^2 \theta}{\partial Y^2}\right) \quad (4)$$

The dimensionless boundary conditions for the flow across a rotating circular cylinder can be written as (see Fig. 1):

At the inlet boundary: $U=1, V=0$ and $\theta=0$

At the exit boundary: $\partial U/\partial X=0, \partial V/\partial X=0$ and $\partial \theta/\partial X=0$

On the surface of the cylinder: $U=-\alpha\sin(\phi), V=-\alpha\cos(\phi)$ and $\theta=1$

The boundary condition on the surface of the cylinder can be implemented by considering wall motion: moving wall and motion: rotational for a particular rotational speed in Fluent.

The above governing equations (1) – (4) when solved using the above boundary conditions yield the primitive variables, i.e., velocity (U and V), pressure (p) and temperature (θ) fields. The local and global characteristics such as local and average Nusselt numbers are obtained using these flow and thermal fields.

3. Numerical details

The computational grid for the problem under consideration is generated by using a commercial grid generator GAMBIT and the numerical calculations are performed in the full computational domain using FLUENT for varying conditions of Reynolds number, Prandtl number and rotation rate. In particular, the O-type grid structure is created here and it consists of non-uniform quadrilateral cells having a total of 24000 grid points in the full computational domain. The grid near the surface of the cylinder is sufficiently fine to resolve the boundary layer around the cylinder. The nearest grid point from the circular obstacle is taken to be at a distance of $0.0015D$, where D is the diameter of the cylinder. The outer boundary is taken to be at a distance of $300D$. The 2-D, steady, laminar, segregated solver is employed here to solve the incompressible flow on the collocated grid arrangement. The second order upwind scheme is used to discretize convective terms of momentum equation, whereas the diffusive term is discretized by central difference scheme.The semi implicit method for the pressure linked equations (SIMPLE) has been used to solve Navier–Stokes and energy equations along with the above noted boundary conditions. A convergence criterion of 10^{-10} is used for continuity, the x- and y-components of Navier–Stokes and energy equations.

3.1 Choices of numerical parameters

In the present study, three non-uniform grids of 18000, 24000 and 32000 cells (with 50, 100 and 200 grid points on the surface of the cylinder and having a first grid point at distances of $0.0018D$, $0.0015D$ and $0.001D$) have been tested for the domain size of $300D$ for the grid resolution study. The percentage relative differences in the values of the total drag coefficient and the average cylinder Nusselt number are found to be less than 4.85

% and 4.6 %, respectively for the highest value of the Reynolds number of 35 and the rotation rate of 5 for the Prandtl number of 100 used in this work. The grid structure of 24000 cells with 200 grid points on the surface of the cylinder and having a first grid point at a distance of $0.0015D$ is used in all the computations reported in this work. Similarly, the domain dependence study is carried out for the two values of the computational domain, i.e., $200D$ and $300D$ for the grid size of 24000 cells with 200 grid points prescribed on the surface of the cylinder and having a first grid point at a distance of $0.0015D$. The percentage differences in the values of the drag coefficient and the average Nusselt number are found to be less than 3.5 % and 3 % for the Reynolds number of 35 and the rotation rate of 5 for the Prandtl number of 100. Thus, the computational domain of 300 times the diameter of the cylinder is used in this work.

4. Results and discussion

In this study, effects of Reynolds and Prandtl numbers around a rotating circular cylinder are examined for Re = 1 - 35 (in the steps of 5) for Pr = 0.7, 1, 10, 50 and 100 for α varying from 0 – 5 (in the steps of 1). The validation of present results, representative isotherm patterns, variation of the local Nusselt number on the surface of the cylinder and the average Nusselt number of the cylinder for the above range of conditions are discussed in the next sub-sections in the steady unconfined flow regime.

4.1 Validation of results

Extensive benchmarking of the present heat transfer results with literature values is carried out here for Re = 10, 20 and 40 for a stationary cylinder ($\alpha = 0$) for Prandtl numbers of 0.7, 1, 50 and 100 (Table 1) and for a rotating cylinder ($\alpha \neq 0$) for Re = 20 and 40 for the Prandtl number of 0.7 (Table 2) in the steady flow regime. The present results of the average Nusselt number for the stationary cylinder are in excellent agreement with the literature values.

Table 1: Comparison of present $\bar{Nu}$ results ($\alpha = 0$) with literature values

Source	Pr = 0.7	Pr = 1	Pr = 50	Pr = 100
	Re = 10			
Present work	1.8371	2.0575	7.0991	8.8611
Bharti *et al.* [7]	1.8623	2.0942	7.1942	8.9942
	Re = 20			
Present work	2.4317	2.7313	9.7518	12.3032
Bharti *et al.* [7]	2.4653	2.7242	9.8642	12.4442
	Re = 40			
Present work	3.2374	3.6506	14.1345	17.9347
Bharti *et al.* [7]	3.2825	3.6842	14.1242	17.9044

For instance, the maximum relative change between the present results and that of the literature values is found to be about 1.75 %. For a rotating cylinder, the maximum change between the present results and that of Paramane and Sharma [18] is found to be less than 4.65 % for varying rotation rates for Re = 20 and 40. Thus, this validates the present numerical solution procedure.

Table 2: Comparison of present $\bar{Nu}$ results with Paramane and Sharma [18]

α	Paramane and Sharma [18]	Present work	Paramane and Sharma [18]	Present work
	Re = 20		Re = 40	
0	2.4189	2.4317	3.2465	3.2374
1	2.3883	2.3994	3.1954	3.1968
2	2.2861	2.3031	3.0115	3.0266
3	2.2248	2.2460	2.9502	2.9642
4	2.2554	2.2768	3.0422	3.0512
5	2.2759	2.3010	3.0115	3.0156
6	2.2248	2.2185	2.4802	2.3658

4.2 Isotherm Patterns

The representative isotherm profiles around the rotating cylinder for various values of rotation rates for the Reynolds numbers of 1, 20 and 35 for Prandtl numbers of 0.7, 50 and 100 are shown in the Figs. 2 – 4 (a - i). It is worth mentioning that no reverse flow in the simulation is observed for the range of conditions studied here. For a stationary cylinder, isotherms have maximum density close to the front surface of the cylinder. This indicates high temperature gradients or in other words, the higher values of local Nusselt number near the front stagnation point on the front surface as compared to other points on the cylinder surface. For a fixed Prandtl number, the density of isotherms close to the rear surface of the cylinder increases on increasing the Reynolds number. This effect can be explained as on increasing the Reynolds number, the recirculation region increases. Similar trend is observed on increasing Prandtl number keeping Reynolds number constant. As the value of Prandtl number increases, the thermal boundary layer becomes thinner which leads to an increase in the temperature gradients close to the rear end. On increasing the value of the rotation rate, the maximum density of isotherms shifts from front surface towards the bottom surface of the rotating cylinder (rotating counter-clock wise) for the fixed Prandtl and Reynolds numbers. It is also observed that isotherms shifts in the direction of rotation of the cylinder and becomes almost vertical at higher values of the rotation rate. However, at Re = 1, Pr = 0.7, slight change in isotherm patterns occurs on increasing the rotation rate. The decay of temperature fields around the cylinder can also be seen in these figures as the value of the Prandtl number increases due to the thinning of the thermal boundary layer. The temperature distributions

presented by way of isotherms can be used to interpret the variation in the local and average heat transfer characteristics with Reynolds number, Prandtl number and rotation rate.

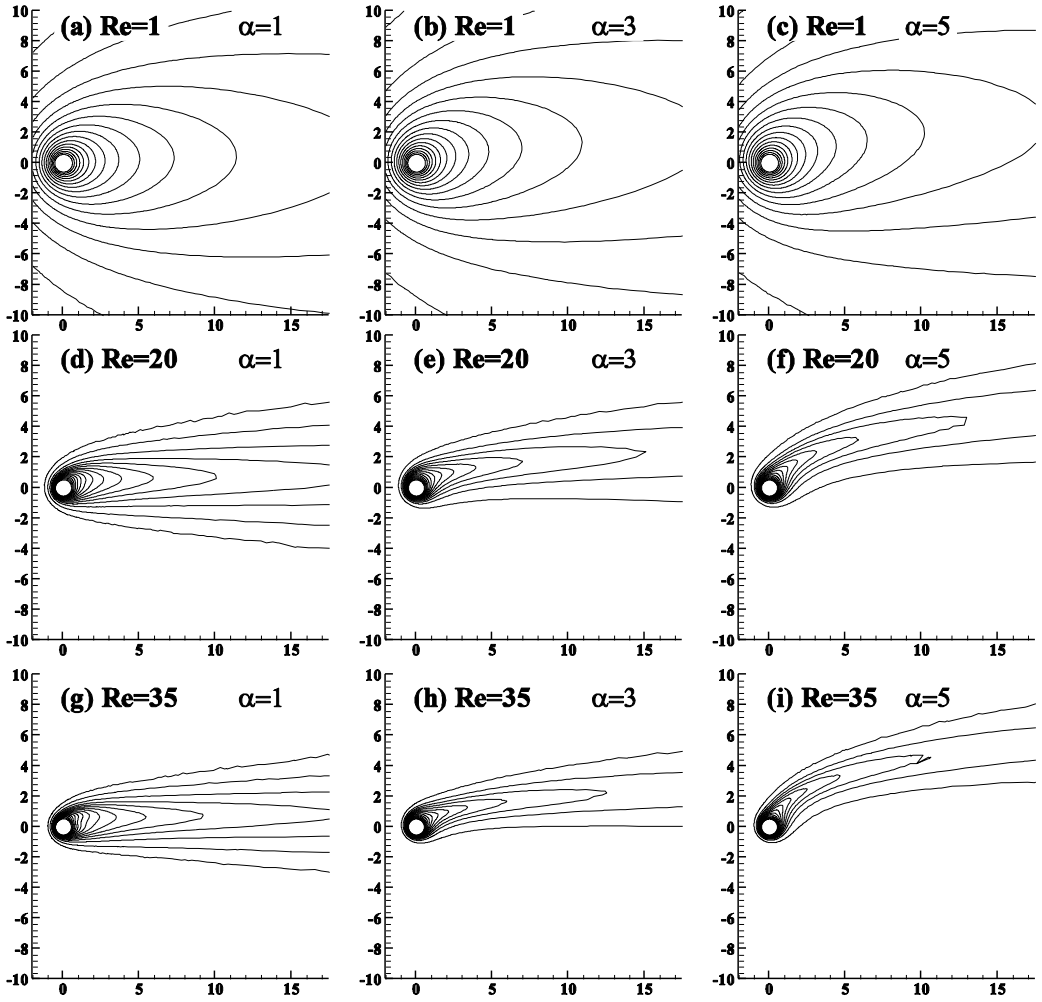

Figure 2: Isotherm profiles at Pr = 1 for varying values of Reynolds number and rotation rate

4.3 Local Nusselt number

Figures 5 (a - *l*) show the variation of the local Nusselt number on the surface of the circular cylinder for different rotation rates (α = 0, 1, 3 and 5) for Prandtl numbers of 0.7, 50 and 100 for Reynolds numbers of 1, 20 and 35. For a stationary cylinder, i.e., at α = 0 (Figs. 5a, e, i), the variation of the local Nusselt number around the cylinder is found to be symmetrical at $\phi = 180^0$. The maximum value of the local Nusselt number occurs at the front stagnation point for all Reynolds and Prandtl numbers studied; whereas the least value occurs at the rear stagnation point for Re = 1. A kink is also observed at the rear end of the cylinder for higher values of Prandtl numbers ($\mathrm{Pr} > 0.7$) and the size of the kink increases as the value of the Prandtl number increases for the fixed value of the Reynolds number. For a rotating circular cylinder, for the low value of the Prandtl number (Pr = 0.7), the maximum in the value of the local Nusselt number shifts in the direction of the rotation and the kink also shifts in the direction of rotation at $\alpha = 1$ (Fig. 5b); however, on further increasing the value

of the rotation rate ($\alpha > 1$), the kink disappears (Figs. 5c, d). On the other hand, for the higher value of the Prandtl number ($\mathrm{Pr} > 0.7$), the shift in the maximum value of the local Nusselt number is more than that of Pr = 0.7 and the slight shift in the kink in the direction of rotation is observed at $\alpha = 1$ (Figs. 5f, j); however, on further increasing the value of the rotation rate ($\alpha > 1$), the local Nusselt number curve becomes smooth and the kink disappears (Figs. 5g, h, k, *l*). On increasing the value of the Prandtl number, the local Nusselt number curve becomes smooth and almost independent of rotation rates at higher rotation rates (Figs. 5g, h, k, *l*). It can also be observed that for the fixed value of the Prandtl number, the value of the local Nusselt number increases with increasing Reynolds number for a particular α; however, the value of the local Nusselt number decreases with increasing rotation rate for the fixed value of the Reynolds number. With increasing value of the Prandtl number, the value of the local Nusselt number increases for the fixed value of the Reynolds number and the rotation rate in the steady regime.

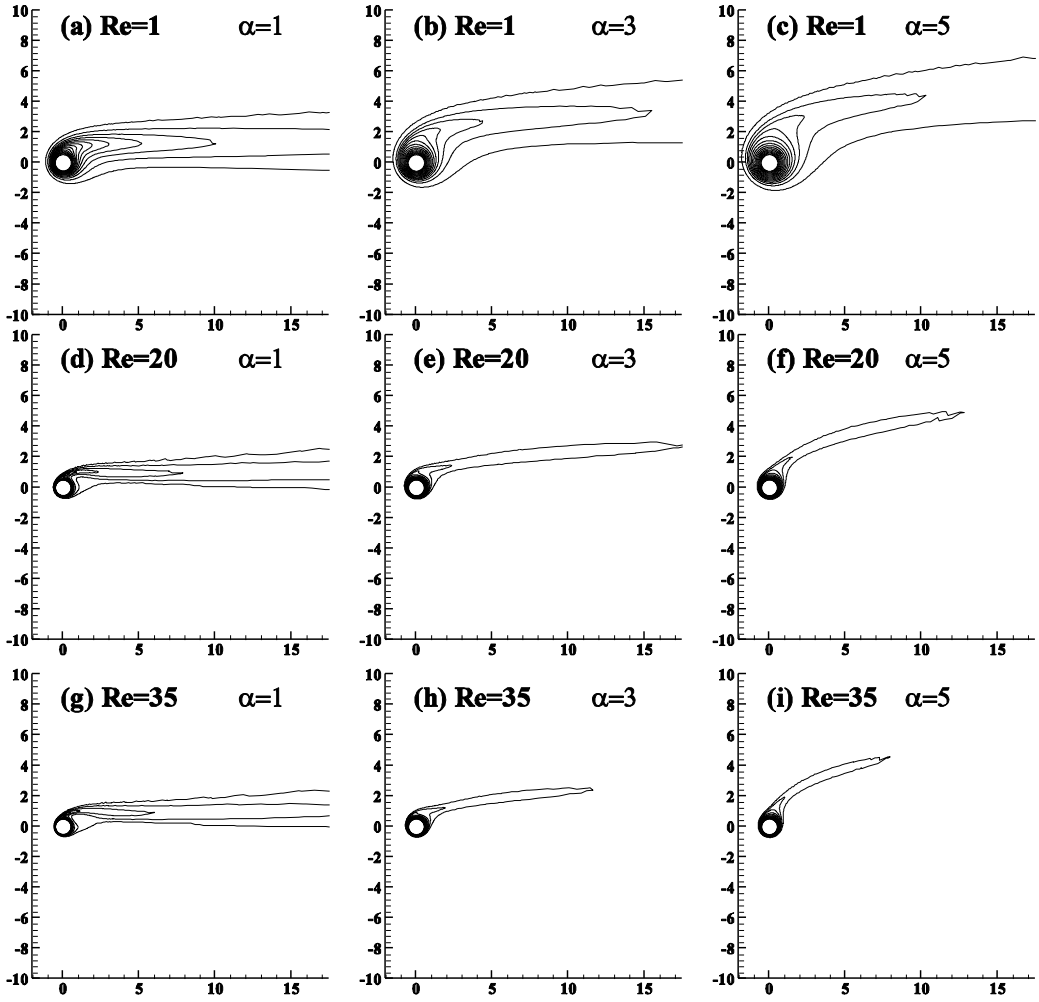

Figure 3: Isotherm profiles at Pr = 50 for varying values of Reynolds number and rotation rate

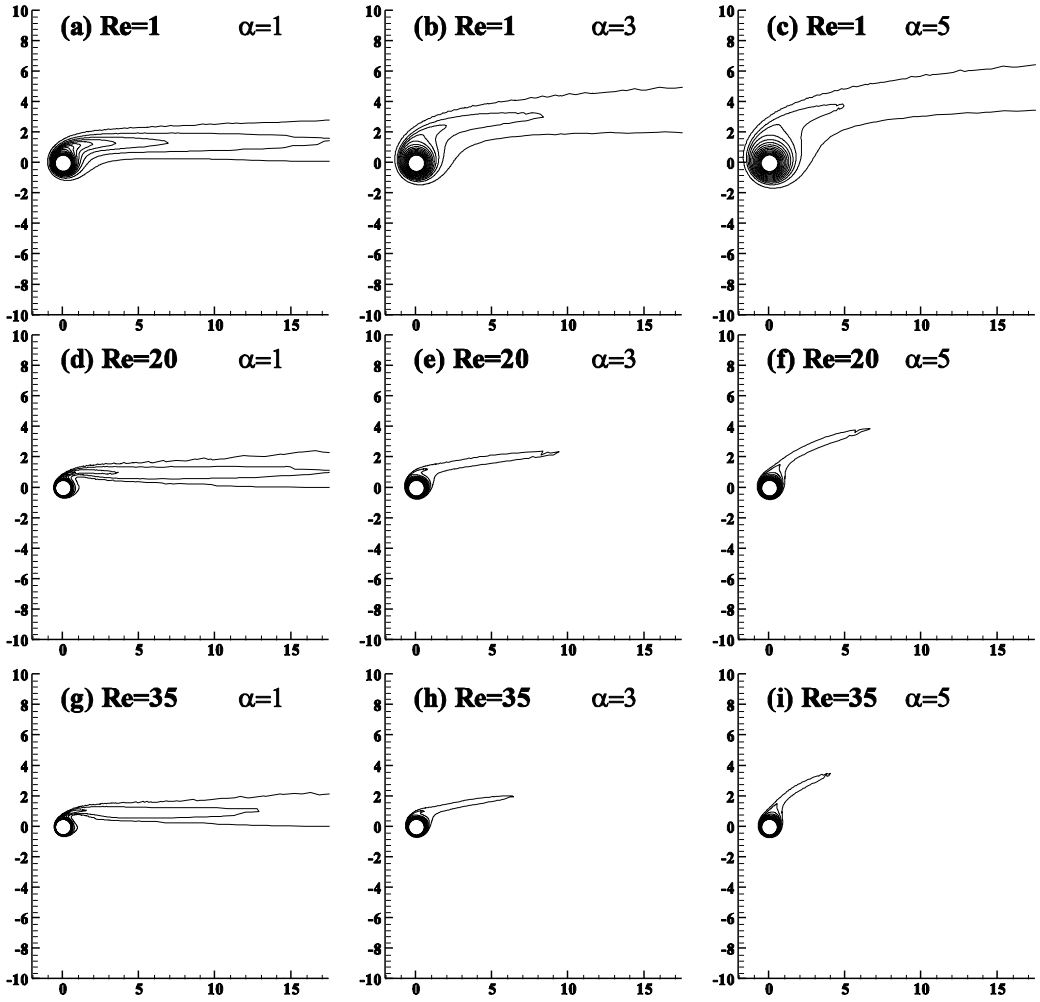

Figure 4: Isotherm profiles at Pr = 100 for varying values of Reynolds number and rotation rate

4.4 Average Nusselt number

The average Nusselt number variation is presented in Figs. 6(a - d) for the Prandtl number range 0.7 - 100 in the steady regime. On increasing the value of the rotation rate, for the fixed value of the Prandtl number, the value of the average Nusselt number decreases for all Reynolds numbers studied here. This is due to the enveloping vortex containing the fluid trapped inside for the decrease in the average Nusselt number with increase in the rotation rate as also explained in [18] for the fixed Prandtl number of 0.7. This enveloping vortex acts as a buffer for heat transfer and limits the heat transfer to only conduction. Further, as the size of this vortex continuously increases with increasing rotation rate, conduction heat transfer decreases thereby reducing the average Nusselt number. For a fixed rotation rate, the value of the average Nusselt number increases with increasing Reynolds number for a fixed Prandtl number. This can be explained as when Reynolds number increases the inertia of flow increases thereby increasing the heat transfer. The decrease in the average Nusselt number is more at higher values of Reynolds and Prandtl numbers as compared to lower values of Reynolds and Prandtl numbers. In other words, at low Reynolds and Prandtl numbers, the

decrease in the average Nusselt number is very slow. On increasing the value of the Prandtl number, the average Nusselt number increases for the fixed value of the Reynolds number for a particular α.

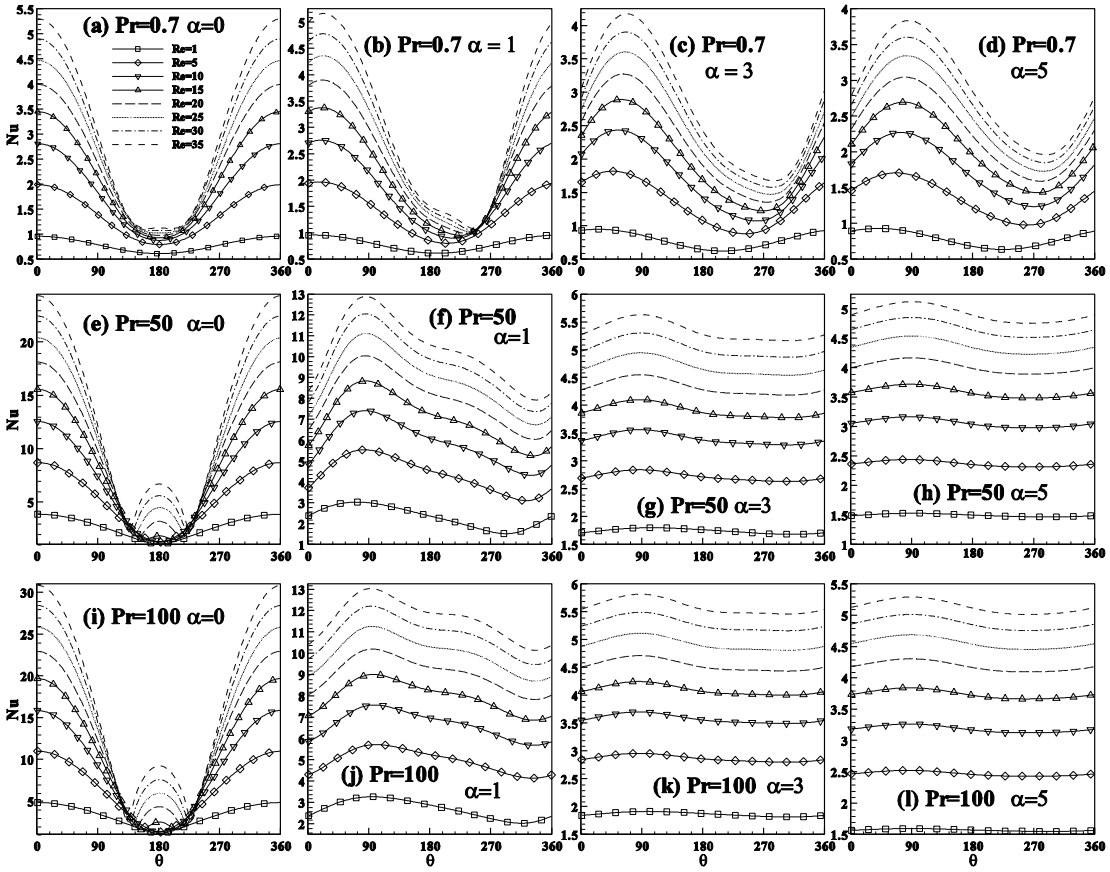

Figure 5: Local Nusselt number variation for Pr = 0.7, 50 and 100 for varying values of Reynolds number and rotation rate

At **Pr = 0.7**: the percentage maximum change in the value of the average Nusselt number (taking reference values to be at α = 0) for the case α = 1 is in the range 0.06 (Re = 1) - 1.34 (Re = 25), for the case α = 2 is in the range 0.24 (Re = 1) - 6.3 (Re = 35), for α = 3 is in the range 0.5 (Re = 1) - 8.34 (Re = 35), for α = 4 is in the range 0.7 (Re = 1) - 6.4 (Re = 20), for α = 5 is in the range 0.9 (Re = 1) - 6.4 (Re = 35).

At **Pr = 1:** the percentage change in the average Nusselt number for the case α = 1 is in the range 0.2 (Re = 1) - 1.5 (Re = 15), for the case α = 2 is in the range 7 (Re = 20) - 15 (Re = 15), for α = 3 is in the range 1.2 (Re = 1) - 11.8 (Re = 35), for α = 4 is in the range 1.8 (Re = 1) - 9.76 (Re = 20), for α = 5 is in the range 2.3 (Re = 1) - 10 (Re = 35).

At **Pr = 10:** the percentage change in the average Nusselt number for the case α = 1 is in the range 3.24 (Re = 1) - 11.9 (Re = 15), for the case α = 2 is in the range 10.24 (Re = 1) – 30 (Re = 15), for α = 3 is in the range 15.86 (Re = 1) - 39.6 (Re = 15), for α = 4 is in the range 20 (Re = 1) - 42 (Re = 15), for α = 5 is in the range 23 (Re = 1) - 42.3 (Re = 15).

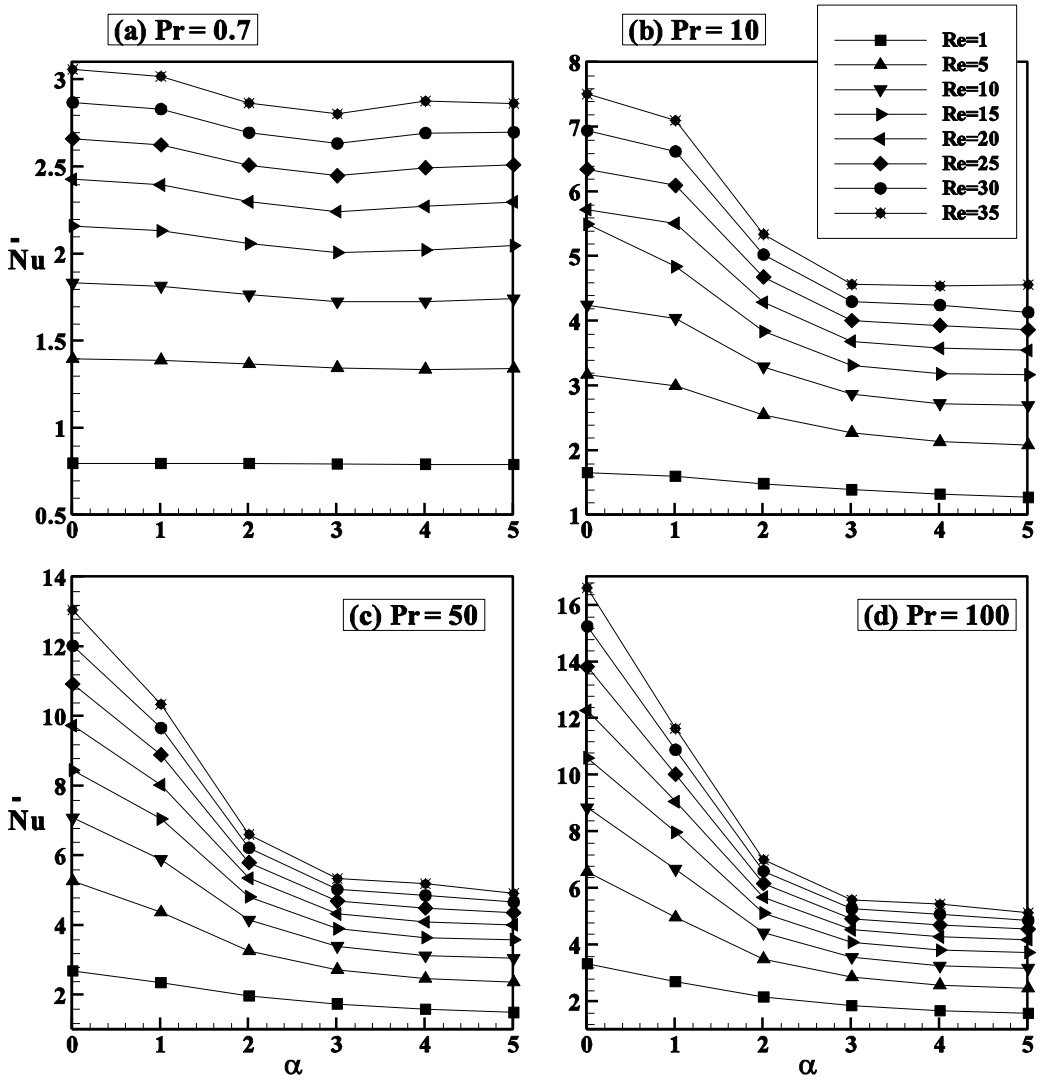

Figure 6: The average Nusselt number variation with increasing α for Pr = 0.7, 10, 50 and 100 for varying Reynolds number

At **Pr = 50:** the percentage change in the average Nusselt number for the case α = 1 is in the range 12.44 (Re = 1) - 20.7 (Re = 35), for the case α = 2 is in the range 26.4 (Re = 1) - 49.3 (Re = 35), for α = 3 is in the range 35 (Re = 1) - 59 (Re = 35), for α = 4 is in the range 40.5 (Re = 1) - 60 (Re = 35), for α = 5 is in the range 44 (Re = 1) - 62.3 (Re = 35).

At **Pr = 100:** the corresponding percentage change in the average cylinder Nusselt number for the case α = 1 is in the range 18.8 (Re = 1) - 29.9 (Re = 35), for the case α = 2 is in the range 35 (Re = 1) - 57.8 (Re = 35), for α = 3 is in the range 44 (Re = 1) - 66.3 (Re = 35), for α = 4 is in the range 49.4 (Re = 1) - 67.2 (Re = 35), for α = 5 is in the range 52.4 (Re = 1) – 69 (Re = 35).

5. Conclusions

In the present study, forced convection heat transfer for varying values of Prandtl number has been studied across a long rotating circular cylinder. The cylinder is rotating at a rotation rate (α) varying from 0 - 5 in the Reynolds number range 1 - 35 and Prandtl number range 0.7 - 100. The representative isotherm patterns are presented and analyzed for the above

range of conditions. For the fixed value of the Prandtl number, the value of the local Nusselt number increases with increasing Reynolds number for the fixed α; however, the value of the local Nusselt number decreases with increasing rotation rate for the fixed value of the Reynolds number. With increasing value of the Prandtl number, the value of the local Nusselt number increases for the fixed value of the Reynolds number and the rotation rate in the steady regime. The average Nusselt number increases with increasing Prandtl number for the fixed value of the Reynolds number for the particular value of α.

Nomenclature

c_p - specific heat of the fluid, [J kg^{-1} K^{-1}]

D - diameter of the circular cylinder, [m]

h - local heat transfer coefficient, [W m^{-2} K^{-1}]

$\bar{h}$ - average heat transfer coefficient, [W m^{-2} K^{-1}]

k - thermal conductivity of the fluid, [W m^{-1} K^{-1}]

Nu - local Nusselt number (= hD/k), [-]

$\bar{Nu}$ - average Nusselt number (= $\bar{h}D/k$), [-]

p^* - pressure, [Pa]

p - non-dimensional pressure (= $p^*/(\rho U_\infty^2)$), [-]

Pr - Prandtl number (= $\mu c_p / k$), [-]

Re - Reynolds number (= $\rho U_\infty D / \mu$), [-]

T_∞ - temperature of the fluid at the inlet, [K]

T_w^* - constant wall temperature at the surface of the cylinder, [K]

t - time, [s]

u - stream-wise velocity, [m s^{-1}]

U_∞ - free-stream velocity, [m s^{-1}]

U - non-dimensional stream-wise velocity (= u/U_∞), [-]

v - cross stream velocity, [m s^{-1}]

V - non-dimensional cross stream velocity (= v/U_∞), [-]

x - stream-wise dimension of coordinates, [m]

X - non-dimensional stream-wise dimension of coordinates (= x/D), [-]

y - cross-stream dimension of coordinates, [m]

Y - non-dimensional cross stream dimension of coordinates (= y/D), [-]

Greek symbols

α - non-dimensional rotation rate (= $D\omega/2U_\infty$), [-]

μ - viscosity of the fluid, [Pa s]

ρ - density of the fluid, [kg m^{-3}]

ϕ - angle measured from the front stagnation point, [degree]

τ - non-dimensional time (= tU_∞ / D), [-]

θ - non-dimensional temperature (= $(T^* - T_\infty)/(T_w^* - T_\infty)$), [-]

ω - constant angular velocity of cylinder rotation, [rad s^{-1}]

Superscripts

***** - dimensional variable

References

[1] Zukauskas, A., Convective Heat Transfer in Cross Flow. In: Zukauskas, A., Kakac, S., Shah, R. K., Aung, W. (Eds): Handbook of Single-Phase Convective Heat Transfer. Wiley, New York, 1987, pp. 6.1 – 6.45

[2] Morgan, V. T., The Overall Convective Heat Transfer From Smooth Circular Cylinders, *Adv. Heat Transfer, 11* (1975) pp. 199 - 264

[3] Dennis, S.C.R., Hudson, J.D., Smith, N., Steady Laminar Forced Convection From a Circular Cylinder at Low Reynolds Numbers, *Phys. Fluids, 11* (1968) pp. 933–940

[4] Chang, M.W., Finlayson, B.A., Heat Transfer in Flow Past Cylinders at Re <150 - Part I. Calculations for Constant Fluid Properties, *Num. Heat Transf., 12* (1987) pp. 179 – 195

[5] Sanitjai, S., Goldstein, R. J., Heat Transfer From a Circular Cylinder to Mixtures of Water and Ethylene Glycol, *Int. J. Heat Mass Transf., 47* (2004) pp. 4785 – 4794

[6] Sanitjai, S., Goldstein, R.J., Forced Convection Heat Transfer From a Circular Cylinder in Crossflow to Air and Liquids, *Int. J. Heat Mass Transf., 47* (2004) pp. 4795–4805

[7] Bharti, R.P., Chhabra, R.P., Eswaran, V., A Numerical Study of the Steady Forced Convection Heat Transfer From an Unconfined Circular Cylinder, *Heat Mass Transf., 43* (2007) pp. 639–648

[8] Badr, H.M., Dennis, S.C.R., Young, P.J.S., Steady and Unsteady Flow Past a Rotating Circular Cylinder at Low Reynolds Numbers, *Comput. Fluids, 17* (1989) pp. 579–609

[9] Ingham D. B., Tang T., A Numerical Investigation into the Steady Flow Past a Rotating Circular Cylinder at Low and Intermediate Reynolds Numbers, *J. Computational Physics, 87 (1990) 91-107.*

[10] Kang, S., Choi, H., Lee, S., Laminar Flow Past a Rotating Circular Cylinder, *Phys. Fluids, 11* (1999) pp. 3312–3321

[11] Stojkovic, D., Breuer, M., Durst, F., Effect of High Rotation Rates on the Laminar Flow Around a Circular Cylinder, *Phys. Fluids, 14* (2002) pp. 3160–3178

[12] Mittal, S., Kumar, B., Flow Past a Rotating Cylinder, *J. Fluid Mech. 476* (2003) pp. 303–334

[13] Panda, Saroj K., Chhabra, R. P., Laminar Flow of Power-Law Fluids Past a Rotating Cylinder, *J. Non-Newt. Fluid Mech.*, 165 (2010) 1442 - 1461

[14] Badr, H.M., Dennis, S.C.R., Laminar Forced Convection From a Rotating Cylinder, *Int. J. Heat Mass Transf., 28* (1985) pp. 253–264

[15] Mahfouz, F. M., Badr, H. M., Heat Convection From a Cylinder Performing Steady Rotation or Rotary Oscillation - Part I: Steady Rotation, *Heat and Mass Transf., 34* (1999) pp. 365-373

[16] Yan, Y. Y., Zu, Y. Q., Numerical Simulation of Heat Transfer and Fluid Flow Past a Rotating Isothermal Cylinder – A LBM Approach, *Int. J. Heat Mass Transf., 51* (2008) pp. 2519–2536

[17] Kendoush, A.A., An Approximate Solution of the Convection Heat Transfer From an Isothermal Rotating Cylinder, *Int. J. Heat Fluid Flow, 17* (1996) pp. 439–441

[18] Paramane, S. B., Sharma, A., Numerical Investigation of Heat and Fluid Flow Across a Rotating Circular Cylinder Maintained at Constant Temperature in 2-D Laminar Flow Regime, *Int. J. Heat and Mass Transf., 52* (2009) pp. 3205–3216

[19] Paramane Sachin B., Sharma Atul, Heat and Fluid Flow Across a Rotating Cylinder Dissipating Uniform Heat Flux in 2D Laminar Flow Regime, *Int. J. Heat Mass Transf., 53 (2010) 4672-4683.*

[20] Nobari M.R.H., J. Ghazanfarian, Convective Heat Transfer from a Rotating Cylinder with Inline Oscillation, *Int. J. Thermal Sciences, 49 (2010) 2026-2036.*

[21] Nemati Hasan, Farhadi Mousa, Sedighi Kurosh, Fattahi Ehsan, Multi- Relaxation-Time Lattice Boltzman Model for Uniform-Shear Flow over a Rotating Circular Cylinder, *Thermal Sci., 2010*, doi: 10.2298/TSCI100827082N.

[22] Yoon H. S., Seo J. H., Kim J. H., Laminar Forced Convection Heat Transfer Around Two Rotating Side-By-Side Circular Cylinder, *Int. J. Heat Mass Transf., 53 (2010) Pages 4525-4535.*

[23] Moshkin Nikolay Pavlovich, Sompong Jakgrit, Numerical Simulation of Flow and Forced Convection Heat Transfer, *Suranaree J. Sci. Technol., 17(1) (2009) 87-104.*